ELECTRON TRAJECTORY CAUSTIC FORMATION RESULTING IN CURRENT HORNS PRESENT IN BUNCH COMPRESSION

T. K. Charles*, D. M. Paganin, School of Physics and Astronomy, Monash University, Australia
M. J. Boland, R. T. Dowd, Australian Synchrotron, Clayton, Australia

Abstract

Current horns are ubiquitous in Free Electron Laser (FEL) bunch compression. In this paper, we analyse the formation of these current spikes and identify the cause as caustic formation in the electron trajectories. We also present a possible solution to avoid or mitigate the current horns from developing through inclusion of sextupole and octupole magnets in the compressor design.

INTRODUCTION

In the bunch compression process we often witness the development of current spikes, or horns, appearing at the head and tail of the beam [1–3]. These current spikes can induce coherent synchrotron radiation (CSR) that can lead to emittance growth [4–6]. The root cause of these current spikes is often attributed to wakefields introducing a third order chirp on the beam [7, 8]. Here, we analyse how these current spikes form.

Here we discuss how these current peaks result from electron trajectories converging in longitudinal position, z as the bunch is compressed. This coalescing of electron trajectories in z results in the greatly enhanced current at the head and tail of the beam. In catastrophe theory terms, this is known as a fold caustic [9, 10].

Caustics are a common occurrence in optics, often spotted as intense reflections in coffee cups and the dancing spots of light in swimming pools. In fact, electron trajectories forming caustics in bunch compression could be considered a corollary to these examples of natural focusing of light in geometrical optics. In both cases, electrons and light rays, the mathematical description of caustics lies within the broader field of catastrophe theory.

FOLDS IN LONGITUDINAL PHASE SPACE

To find the electron trajectories that coalesce to form caustics, we need to look at the beam in the z–s plane, where z is the longitudinal position within the bunch and s is the position along the accelerator. Whilst this is not a common coordinate plane to consider the evolution of the beam, we know the current horns appears as electrons piling up at the same z positions as we move through the compressor in s.

Considering the z–s plane, we can derive an expression for the electron trajectories as they evolve with s from the initial longitudinal positions, z_i. This leads to the equation where the final longitudinal position z_f is,

$$z_f(s) = \left(\frac{R_{56}\delta + T_{566}\delta^2}{l_{bc}} \right) s + z_i . \tag{1}$$

where R_{56}, T_{566} and U_{5666} are the first, second and third order longitudinal dispersion, δ is the relative energy deviation and l_{bc} is the length length of the compressor.

This expression assumes that the longitudinal dispersion remains constant over the compressor, which is an inaccurate statement but will however produce the same output distribution at the end of the compressor when compared to an expression that includes how R_{56} varies with s.

At the beginning of the bunch compressor, the longitudinal phase space distribution can be modeled as a third order polynomial in z_i,

$$\delta = c_1 z_i^3 + c_2 z_i^2 + c_3 z_i . \tag{2}$$

where c_1, c_2, and c_3 are fitted parameters. These higher order terms are a necessary condition in order to produce the current spikes we witness. These higher order terms may be introduced through wakefields, space charge forces or other non-linear effects. Figure 1 shows a distribution taken from an Elegant simulation [11], of an x-band FEL design [12, 13], taken just before the bunch enters the second bunch compressor (BC2), and includes the fitted expression of Eq. 2.

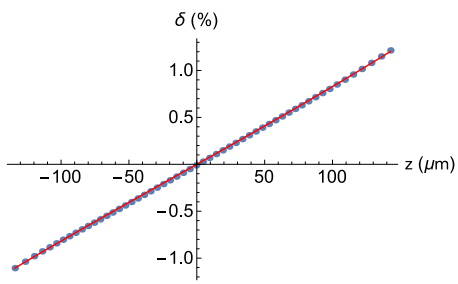

Figure 1: Elegant distribution taken before BC2, with a fit of the form, $\delta = c_1 z_i^3 + c_2 z_i^2 + c_3 z_i$.

Equation (1) has been plotted in Fig. 2 using initial z_i values from the fitted expression for δ shown in Fig. 1. Figure 2 shows the bunch compression over the length of the chicane, and Fig. 3 shows a closer view of the caustics. In Fig. 3, the caustics are visible, with a high density of electrons at the extreme values of z. i.e. the head and the tail of the bunch.

When the electron trajectories are projected onto the z axis, the resulting histogram agrees with the the Elegant produced current profile at the end of the compressor (see in Fig. 4). This double-horned current profile, which here

* tessa.charles@monash.edu

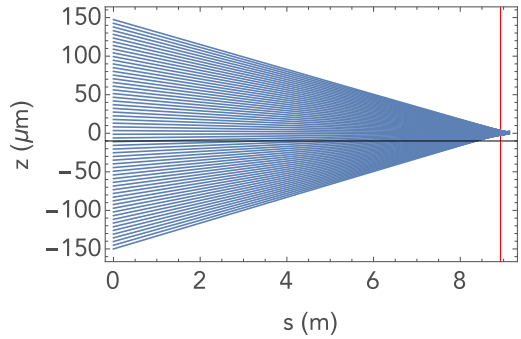

Figure 2: Electron trajectories through a chicane in z–s plane, where the vertical red line at 8.928 m is the end of the compressor.

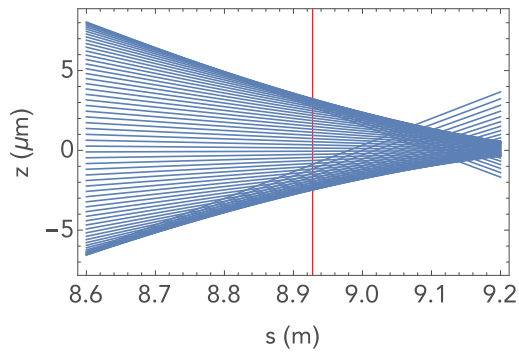

Figure 3: Electron trajectories near the end of the chicane (vertical red line at 8.928 m), showing how the electron trajectories overlapping in a caustic at the head and the tail of the bunch.

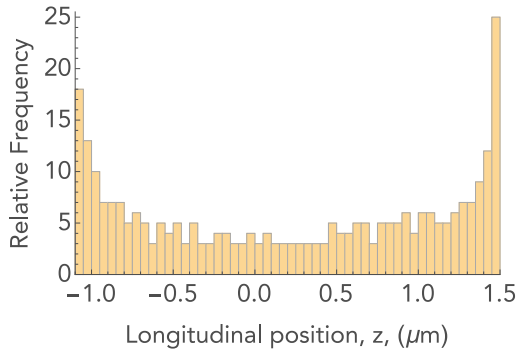

(a) Histogram showing density of electrons after being transported through a bunch compressor, corresponding to the longitudinal positions marked by the vertical line in Fig. 2.

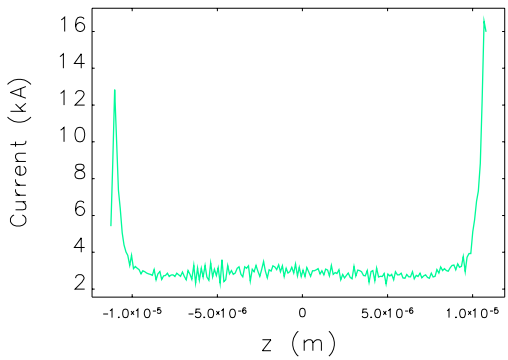

(b) Current profile produced with Elegant simulation.

Figure 4: Current profile showing current spikes at the head and tail of the bunch.

we associate with caustics, is ubiquitous in FEL bunch compression [1, 2]. Single-horned current profiles can also be produced through a magnetic chicane, such as those seen in [14–17]. Figure 5 demonstrates a single-horn distribution resulting from a caustic forming at one end of the bunch.

EXPRESSION FOR THE CAUSTIC REGIONS

Starting with Eq. (1) we can derive an expression for the caustic to be,

$$R_{56}s\frac{d(\delta(z))}{dz}\bigg|_{z=z_i} + T_{566}s\frac{d}{dz}\left(\delta^2(z)\right)\bigg|_{z=z_i} + \ldots$$
$$U_{5666}s\frac{d}{dz}\left(\delta^3(z)\right)\bigg|_{z=z_i} + l_{BC} = 0. \quad (3)$$

Assuming we are only concerned if caustics form by the end of the chicane, then we can set $s = l_{BC}$. Also for a standard magnetic chicane, we assume $T_{566} = -3/2R_{56}$ and $U_{5666} = -2R_{56}$.

The parametric form for the set of caustic points $(\tilde{z},\tilde{s})$ in the z–s plane, parameterized by z_i is,

$$\tilde{z}(z_i) = \frac{\frac{3}{2}\delta^2(z_i) - \delta(z_i)}{\delta'(z_i)(1-3\delta(z_i))}$$
$$\tilde{s}(z_i) = \frac{-l_{BC}/R_{56}}{\delta'(z_i)(1-3\delta(z_i))}. \quad (4)$$

Figure 6 shows the parametric Eq. (4) over the electron trajectories, mapping out the family of trajectories that form the caustics.

DISCUSSION

Figures 3 and 5 show the electron trajectories resulting in fold caustics. It should be noted that mathematical formulation of the set of Eq. (4) is applicable for all high-order catastrophes such as cusps, swallowtails, elliptic umbilics, and hyperbolic umbilics.

If for a set of parameters c_1, c_2, c_3, R_{56}, T_{566}, and U_{5666} there exists any solutions to Eq. (3), we can expect to encounter enhanced current peaks. The greater the number of solutions, the more intense the peaks. We can attempt to find a set of parameters for which the left-hand-side of Eq. (3) never equals zero, and therefore no caustics will form. This requires the ability to manipulate either the coefficients

ISBN 978-3-95450-147-2

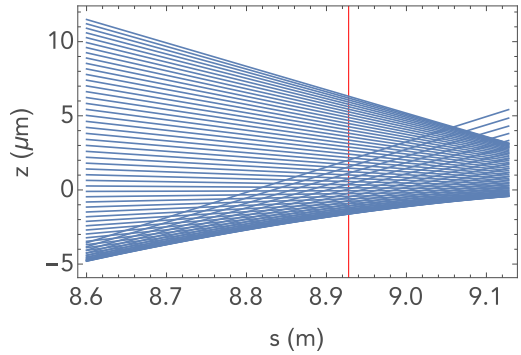

(a) Electron trajectories where the vertical solid red line indicates the end of the compressor.

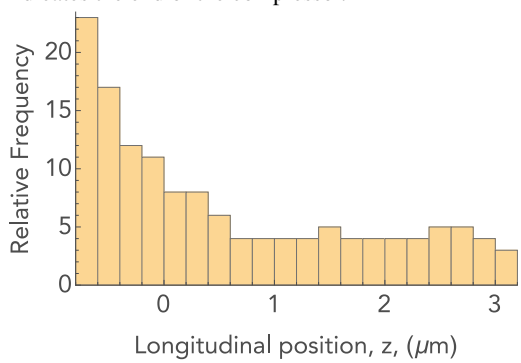

(b) Histogram showing the density of electrons after begin transported through a bunch compressor (corresponding to the red line above).

Figure 5: Single-horn current profile produced by fold caustic forming at the tail of the bunch.

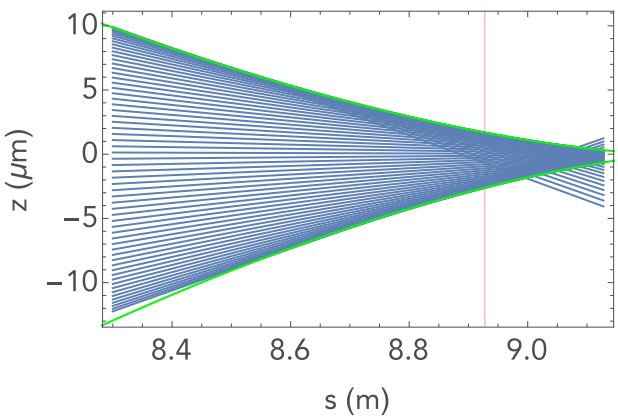

Figure 6: Electron trajectories with the caustic expressions (Eq. (4)) in green.

describing the longitudinal phase space at the entry of the compressor, i.e. c_1, c_2 and c_3; or ability to manipulate R_{56}, T_{566}, and U_{5666}. Given the small but vital role the coefficients of the higher order terms of δ play, it would be difficult to vary these parameters in a controlled manner. Furthermore if we assume that wakefields are at least in part responsible for these coefficients, then we must concede the difficulty in changing these parameters due to the dependency of wakefields on beam charge and structure geometry.

For a standard standard magnetic chicane, $T_{566} = -3/2R_{56}$, and $U_{5666} = -2R_{56}$ however if we design a compressor that utilises optical linearization, then we can attempt to find a combination for R_{56}, T_{566} and U_{5666} for which there is no solutions to Eq. (3). An example of this is shown in Fig. 7 where the trajectories from Fig. 3 are unfolded through changing R_{56} from -12.00 mm to -12.22 mm, T_{566} from 18.0 mm to 9.9 mm, and U_{5666} from 24.0 mm to 2.45 m. This allows the caustics to be completely unfolded and therefore eliminates the associated current horns whilst maintaining the final bunch length, but requires a very large value of U_{5666}. Figure 8 shows the histograms of the trajectories (i.e. current) at the end of the chicane corresponding to Fig. 3 and Fig. 7.

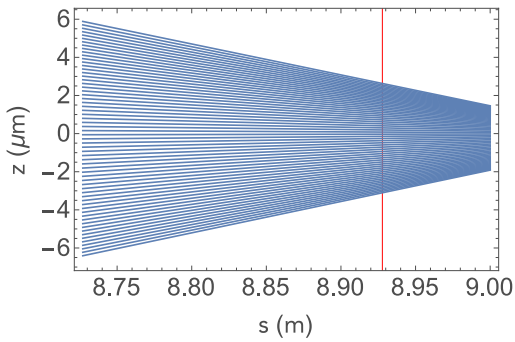

Figure 7: Unfolding the caustics present in Fig. 3, achieved through altering R_{56}, T_{566}, and U_{5666}.

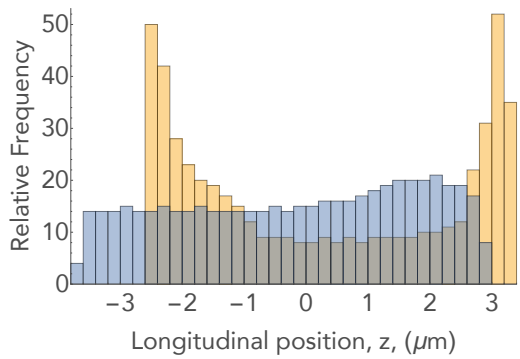

Figure 8: Histograms of the trajectory density at the end of the chicane corresponding to the red vertical line in Fig. 3 (yellow) and Fig. 7 (blue). The blue histogram shows the result of unfolding caustics on the current profile.

CONCLUSION

This paper shows how caustics of electron trajectories can be used to completely describe the double-horn current profile often encountered in bunch compression. Using the analytical expressions derived, compressors may be able to be designed to avoid caustics using optical linearization to independently vary R_{56}, T_{566}, and U_{5666}.

REFERENCES

[1] Arthur, J. *et al.*, "Linac Coherent Light Source (LCLS) Conceptual Design Report", SLAC-0593, April (2002),

[2] Zhou, F. Bane, K. Ding, Y. Huang, Z. Loos, H. Raubenheimer, T. Phys. Rev. ST Accel. Beams **18**, 050702 (2015).

[3] Emma, P. "Accelerator Physics challenges of X-ray FEL SASE Sources" Proc. of EPAC 2002, Paris, France, June 2002.

[4] Braun, H. Corsini, R. Groening, L. Zhou, F. Kabel, A. Raubenheimer, T. Li, R. Limberg, T. Phys. Rev. ST Accel. Beams **3**, 124402 (2000).

[5] Borland, M. Phys. Rev. ST Accel. Beams **4**, 070701 (2001).

[6] Li, R. Phys. Rev. ST Accel. Beams **2**, 024401 (2008).

[7] Di Mitri, S. Cornacchia, M. Phys. Rep. **539**, 1–48 (2014).

[8] Bane, K. L. F. Raubenheimer, T. O. Seeman, J. T. "Electron Transport of a Linac Coherent Light Source (LCLS) Using the SLAC Linac", Proc. IEEE 1993 Particle Accelerator Conference, Washington, DC, May 1993

[9] Berry, M. V. Upstill, C. Prog. **8**, 257–346 (1980).

[10] Nye, F. Y. *Natural Focusing and Fine Structure of Light Caustics and Wave Dislocations*, (Taylor & Francis, Philadelphia, 1999).

[11] M. Borland, "elegant: A Flexible SDDS-Compliant Code for Accelerator Simulation", Advanced Photon Source LS-287, September 2000.

[12] M. Boland et. al., "Plans for an Australian XFEL Using a CLIC X-Band Linac", Proc. of IPAC14, Dresden, Germany, July 2014, THPME081

[13] A. Aksoy et. al., "FEL Proposal Based on CLIC X-Band Structure", Proc. of FEL2014, Basel, Switzerland, August 2014, MOP062

[14] Marchetti, B. Krasilnikov, M. Stephan, F. Zagorodnov, I. Physics Procedia **52**, 80-89 (2014).

[15] Huang, S. Ding, Y. Huang, Z. Qiang, J. Phys. Rev. ST Accel. Beams **17**, 120703 (2014).

[16] Dohlus, M. Flöttmann, K. Kozlov, O. S. Limberg, T. Piot, Ph Saldin, E. L. Schneidmiller, E. A. Yurkov, M. V. Nucl. Instr. Meth. Phys. Res. A **530**, 3 (2004).

[17] Werin, S. Thorin, S. Eriksson, M. Larsson, J. Nucl. Instr. Meth. Phys. Res. A **301**, 98-107 (2009).

ISBN 978-3-95450-147-2